Conf-940553--82

UCRL-JC-115352
PREPRINT

Evaluation of Thermo-Hydrological Performance in Support of the Thermal Loading Systems Study

Thomas A. Buscheck
John J. Nitao
Steven F. Saterlie

This paper was prepared for submittal to the
American Nuclear Society
International High Level Radioactive Waste Management Conference
Las Vegas, Nevada
May 22–26, 1994

January 1994

Contents

Evaluation of Thermo-Hydrological Performance in Support of the Thermal Loading Systems Study

Thomas A. Buscheck and John J. Nitao
Earth Sciences Department, L-206, P.O. Box 808
Lawrence Livermore National Laboratory, Livermore, CA 94551
telephone: (510) 423-9390, (510) 423-0297

Steven F. Saterlie
TRW Environmental Safety Systems
101 Convention Center Drive, Suite P-110/Mailstop 423
Las Vegas, NV 89109
telephone: (702) 794-5376

Abstract

Heat generated as a result of emplacing spent nuclear fuel will significantly affect the pre- and post-closure performance of the Mined Geological Disposal System (MGDS) at the potential repository site in Yucca Mountain. Understanding thermo-hydrological behavior under repository thermal loads is essential in (a) planning and conducting the site characterization and testing program, (b) designing the repository and engineered barrier system, and (c) assessing performance. The greatest concern for hydrological performance is sources of water that would contact a waste package, accelerate its failure rate, and eventually transport radionuclides to the water table. The primary sources of liquid water are: (1) natural infiltration, (2) condensate generated under *boiling conditions*, and (3) condensate generated under *sub-boiling conditions*. Buoyant vapor flow, occurring either on a sub-repository scale or on a mountain scale, may affect the generation of the second and third sources of liquid water. A system of connected fractures facilitates repository-heat-driven gas and liquid flow as well as natural infiltration. With the use of repository-scale and sub-repository-scale models, we analyze thermo-hydrological behavior for Areal Mass Loadings (AMLs) of 24.2, 35.9, 55.3, 83.4, and 110.5 MTU/acre for a wide range of bulk permeability. We examine the temporal and spatial extent of the temperature and saturation changes during the first 100,000 yr. We also examine the sensitivity of mountain scale moisture redistribution to a range of AMLs and bulk permeabilities. In addition, we investigate how boiling and buoyant, gas-phase convection influence thermo-hydrological behavior in the vicinity of emplacement drifts containing spent nuclear fuel. The effort was done in support of a thermal loading systems study being performed to evaluate the impact of various thermal loads on the MGDS.

I. Introduction

The U.S. Department of Energy is investigating the suitability of Yucca Mountain as a potential site for the nation's first high-level nuclear waste repository. The site consists of a series of fractured, nonwelded to densely welded tuff units and is located about 120 km northwest of Las Vegas, Nevada, in an area of uninhabited desert.[1] The potential repository location is in Topopah Spring moderately to densely welded tuff, approximately 350 m below the ground surface and 225 m above the water table.[2] Favorable aspects of Yucca Mountain relate primarily to its arid nature, which results in unsaturated conditions at the potential repository horizon.

Heat generated as a result of emplacing spent nuclear fuel (SNF) will play a significant role in the pre- and post-closure performance of the Mined Geological Disposal System (MGDS) at the potential repository site in Yucca Mountain. Understanding the effects of thermal loading on the MGDS will be essential to (1) the design of a repository and engineered barrier system that will meet the necessary requirements, and (2) the demonstration, with adequate confidence, that the MGDS meets regulatory compliance. Achieving an understanding of the effects of thermal loading will require integration of detailed modeling studies, a comprehensive testing and characterization program, and performance assessments. The purpose of this paper is to discuss the modeling and analysis of thermo-hydrological behavior at Yucca Mountain that was conducted in support of the 1993 Thermal Loading Systems Study.[3]

This paper examines the effects of repository-heat-driven hydrothermal flow in Yucca Mountain over a wide range of thermal loading conditions in the repository. In the failure scenario of greatest concern, water would contact a waste package (WP), accelerate its

failure rate, and eventually transport radionuclides to the water table. Analyses have shown that the only significant source of mobile liquid water is from fracture flow, originating from:

(1) meteoric sources,

(2) condensate generated under *boiling conditions*, and

(3) condensate generated under *sub-boiling conditions*.

The first source of liquid water arises from the ambient system, while the second and third sources are generated by repository heat. Buoyant vapor flow, occurring either on a sub-repository scale or on a mountain scale, may play an important role in the generation of the second and third sources of liquid water. The likelihood of buoyant vapor flow generating significant quantities of condensate depends on whether fracture networks result in a bulk permeability, k_b, that is sufficiently large and sufficiently connected over the length scales at which buoyant convection occurs.[4] Zones of sharply contrasting k_b also influence condensate generation and drainage under both boiling and sub-boiling conditions. Of particular concern are conditions that promote the focusing of vapor flow and condensate drainage. Whether this focusing may result in persistent dripping onto WPs depends on the degree of heterogeneity of fracture permeability and connectivity, and the local thermal loading conditions.[4]

In addition to the effect of repository heat on generating vapor and condensate flow, heat may also change the properties of the fractured rock. Repository-heat-driven geochemical or geomechanical changes may, under some situations, alter hydrological properties (e.g., k_b) and transport properties (e.g., retardation factor, K_d). These changes may either improve or degrade waste containment and isolation, depending on where and when they occur. It will be necessary to understand and quantify these processes to be able to account for their impact on hydrothermal behavior and the performance of the MGDS.

The models used in this study are similar to those used in preceding studies.[4–8] As in past work,[4–8] we use the term Areal Mass Loading (AML) as a synonym for thermal loading conditions. Therefore, a high thermal loading case is referred to as a high-AML case and a low thermal loading case as a low-AML case. For a given burnup [expressed as megawatt-days per metric ton of initial heavy metal (MWd/MTU)], the most useful macroscopic thermal loading parameter in analyzing long-term thermal performance is the AML [expressed in metric tons of uranium per acre (MTU/acre)]. Generally, early-temperature performance (including the peak temperature, T_{peak}) is sensitive to the age of SNF, while the duration of the boiling period, t_{bp}, and post-boiling-period thermal performance are determined by the AML and are insensitive to SNF age. Consequently, we prefer using AML to identify the thermal loading conditions rather than the Areal Power Density [(APD) expressed in kW/acre].

Because of the widespread interest in the spatial and temporal extent of the effects of repository heat, this report emphasizes the details of the perturbed temperature and saturation distributions for a wide range of AMLs. Less emphasis is placed on describing the thermo-hydrological flow processes and regimes. The reader is encouraged to read Ref. 9 for a more thorough discussion of these processes and regimes.

II. Thermal Loading Strategies

The extent to which the three major sources of fracture flow at Yucca Mountain may impact waste package integrity, waste-form dissolution, and radionuclide migration is critically dependent on site conditions as well as on the thermal loading strategy that will eventually be adopted for the MGDS. With respect to repository-heat-driven, thermo-hydrological performance, there are three primary thermal loading strategies (or options). These three strategies are best framed as three fundamental questions:

(1) Can the thermal load be limited and distributed such that it has a negligible impact on hydrological performance?

(2) For intermediate thermal loads, will the impact of thermo-hydrological processes and our understanding of those processes allow us to demonstrate that the MGDS meets regulatory compliance?

(3) For higher thermal loads, which could generate extended-dry conditions, will the impact of thermo-hydrological processes and our understanding of those processes allow us to demonstrate that the MGDS meets regulatory compliance?

The goal of the first thermal loading strategy is to minimize the hydrological impact of repository heat so that the primary concern in assessing hydrological performance is the ambient hydrological system. Therefore, this strategy requires that (1) we demonstrate that repository heat has a negligible impact on hydrological performance, and (2) the behavior of the ambient hydrological system and our understanding of that behavior are sufficient to demonstrate that the MGDS meets regulatory compliance. The motivation for this strategy is to avoid any potentially adverse effects of repository heat.

The goal of the third thermal loading strategy is to demonstrate that, for some period of time, repository heat is capable of dominating the ambient system with above-boiling conditions surrounding the repository. Ideally, this would result in (1) the absence of liquid water in the vicinity of the waste packages as long as boiling persists, and (2) the continuation of sub-ambient liquid saturation conditions for some time following the above-boiling period without incurring adverse effects that may offset the benefits of dry-out. The primary motivations for this strategy are to (a) minimize the sensitivity of repository

performance to hydrological variability, (b) extend the period of radionuclide containment in the engineered barrier system, and, (c) during the period of radionuclide migration, reduce two factors: the probability of water contacting waste packages, and the flow rates associated with transport.

The second thermal loading strategy falls between the first and third strategies. All three strategies require an adequate understanding of both the ambient hydrological system and how heat perturbs fluid flow in that system.

It is important to note that what effectively constitutes a "cold," ambient-system-dominated repository or a "hot," extended-dry repository is not well understood. Presently, we lack adequate knowledge of ambient site conditions to define where the transitions from cold to intermediate or from intermediate to hot thermal loads occur. We have analyzed how site conditions will influence the determination of these transitions.[4,9] In particular, the influence of buoyant, gas-phase convection and how hydrogeological heterogeneity may focus vapor and condensate flow are critical to determining what thermal loads are sufficiently "cold" to render hydrothermal impacts of repository heat as negligible. The influence of these processes will also largely determine what thermal loads are sufficiently "hot" (or whether any such thermal loads exist) to allow us to demonstrate that extended-dry conditions will prevail for some time in the vicinity of waste packages.

Generally speaking, site conditions that are beneficial to a "cold" repository also benefit the performance of a "hot" repository. If we find that the bulk permeability is too small to promote significant buoyant, gas-phase flow and that heteregeneity does not result in significant focusing of vapor flow and condensate drainage, it may be possible to demonstrate that a sub-boiling repository has a negligible impact on the ambient hydrological system. These same site conditions are also beneficial for extending the period of above-boiling temperatures and, during that time, minimizing the presence of mobile liquid water in the vicinity of waste packages.

III. Numerical Models, Physical Data, and Assumptions

III.A V-TOUGH Hydrothermal Flow Code

All hydrothermal calculations in this study were carried out using the V-TOUGH (vectorized transport of unsaturated groundwater and heat) code.[10] V-TOUGH is Lawrence Livermore National Laboratory's enhanced version of the TOUGH code, which was developed at Lawrence Berkeley Laboratory by Pruess.[11] V-TOUGH is a multidimensional numerical simulator capable of modeling the coupled transport of water, vapor, air, and heat in fractured porous media. Our models include boiling and condensation effects, the convection of latent and sensible heat, and thermal radiation.

III.B Equivalent Continuum Model

Because of the impracticality of discretely accounting for all of the fractures at Yucca Mountain, it was necessary to account for fractures using the equivalent continuum model (ECM). The assumption of *capillary pressure and thermal equilibrium between* fractures and matrix allows the fracture and matrix properties to be pore-volume-averaged into an equivalent medium. The bulk porosity, ϕ_b, bulk saturation, S_b, and bulk hydraulic conductivity, K_b, of the equivalent medium are given by:

$$\phi_b = \phi_f + (1 - \phi_f)\phi_m \tag{1}$$

$$S_b = \frac{S_f\phi_f + S_m(1 - \phi_f)\phi_m}{\phi_f + (1 - \phi_f)\phi_m} \tag{2}$$

$$K_b = K_m(1 - \phi_f) + K_f\phi_f \tag{3}$$

where ϕ_m, S_m, ϕ_f, and S_f are the porosity and saturation of the matrix and fractures, respectively, and K_m and K_f are the hydraulic conductivities of the matrix and fractures. Because of the small K_m in the unsaturated zone (UZ), K_b is almost completely dominated by K_f and ϕ_f for most fracture spacings and permeabilities.

III.C Thermo-Hydrological Properties

All major hydrostratigraphic units in the UZ at Yucca Mountain are included in the models.[3,12] The hydrostratigraphic profile employed here has been used in previous modeling studies.[3,6-9,13] The wet and dry thermal conductivity, K_{th}, data were obtained from the Reference Information Base (RIB).[14] In this study we use the RIB Version 4 K_{th} values. We assume the steady-state liquid saturation profile obtained for a net recharge flux of 0 mm/yr, which yields a repository horizon saturation of 68%.[13]

For the primary suite of calculations, a uniform fracture permeability is assumed. Because the bulk permeability, k_b, is dominated by the fracture permeability, this assumption yields a k_b distribution that is nearly uniform. The reference case assumes a k_b of 2.8 $\times 10^{-13}$ m^2 (280 millidarcy), which is equivalent to three 100-μm fractures per meter. We also considered the following values of k_b: 1 millidarcy (three 15-μm fractures per meter), 10 millidarcy (three 33-μm fractures per meter), 84 millidarcy (three 68-μm

fractures per meter), 1 darcy (three 153-μm fractures per meter), 10 darcy (three 330-μm fractures per meter), 40 darcy (one 781-μm fracture per meter), 84 darcy (one 1000-μm fracture per meter), and 168 darcy (one 1260-μm fracture per meter).

III.D Initial and Boundary Conditions

The vertical temperature, T, distribution in the models is initialized to correspond to the nominal geothermal gradient in the region. The atmosphere at the ground surface is represented by a constant-property boundary, with T and gas-phase pressure, p_g, fixed at 13°C and 0.86 atm, respectively. The relative humidity at the ground surface is fixed so that it is in thermodynamic equilibrium with the initial saturation conditions at the top of the TCw unit (the uppermost unit in our models). Therefore, under initial (ambient) saturation and temperature conditions, there is no mass flux of water vapor between the atmosphere and upper TCw.

We conducted our repository-scale calculations with an unsaturated zone/saturated zone (UZ-SZ) model that explicitly includes hydrothermal flow in the upper 1000 m of the SZ. Conductive and convective heat flow, including buoyancy flow, are modeled in the SZ. Because the RIB[14] lacks thermal property and hydrologic data below the PPw unit (the lowermost unit in our UZ model), we assumed that the PPw data were applicable to the upper 1000 m of the SZ (down to the lower boundary of the UZ-SZ model). The lower boundary of the UZ-SZ model has a constant temperature of 53.5°C and a fixed pressure corresponding to the hydrostatic pressure and temperature profile of the upper 1000 m of the SZ.

In some of the previous work,[6] it was assumed that because of the large fracture permeability, buoyant convective mixing in the saturated zone (SZ) results in it acting as a heat sink. The large k_h and storativity of the SZ were also assumed to result in the water table being at a fixed depth. For the drift-scale calculations reported here, we also assume that the water table has a fixed depth (z = 568.1 m) and a constant temperature (31°C). The constant-temperature assumption causes the water table to act as a heat sink. Because this model does not explicitly model hydrothermal flow in the SZ, it is called the "UZ" model. In comparing the UZ model with the UZ-SZ model, we found that, for the first 1000 yr, repository temperatures are insensitive to the treatment of heat flow at the water table.[7,8] Because the primary use of the drift-scale model, which is described below, is to examine sub-repository-scale thermo-hydrological behavior during the first 1000 yr, the constant-temperature water table assumption does not significantly affect the interpretation of our results. The initial temperature and saturation at the repository horizon in both the UZ and UZ-SZ models are 23.5°C and 68%, respectively.

III.E Repository-Scale Models

In conducting our modeling studies, we have represented the repository at several different scales. The repository-scale models assume radial symmetry about the center of the repository and represent the repository as a disk-shaped heat source with a uniformly distributed thermal load over the heated area of the repository. Because of their radial symmetry, these models assume areally uniform thermo-hydrological properties. Layered heterogeneity (i.e., property variability that occurs in the vertical direction) can be represented by these models. We modeled repository areas of 570, 744, 1139, 1755, and 2598 acres. For 63,000 MTU of SNF, these repository areas correspond to AMLs of 110.5, 83.4, 55.3, 35.9, and 24.4 MTU/acre. For 22.5-yr-old SNF, these AMLs correspond approximately to APDs of 114, 86, 57, 37, and 25 kW/acre, respectively. The repository-scale models are well suited for representing mountain-scale behavior, such as mountain-scale, buoyant, gas-phase convection. These models employ a relatively fine gridblock spacing at the outer perimeter of the repository to more accurately account for the effect of edge-cooling. We assume a Youngest Fuel First (YFF) SNF receipt scenario with a 10-yr cutoff for the youngest fuel. This scenario is referred to as YFF(10). We account for, in yearly increments, the emplaced inventory of boiling water reactor (BWR) WPs, containing 40 assemblies per WP, and pressurized water reactor (PWR) WPs, containing 21 assemblies per WP. The waste receipt schedule was determined by King.[15] For the 110.5-MTU/acre case, we considered the following values of k_h: 1, 10, 84, and 280 millidarcy; and 1, 10, 40, and 84 darcy. For the 24.4-, 35.9-, 55.3-, and 83.4-MTU/acre cases, we considered k_h values of 280 millidarcy and 1, 10, 40, and 84 darcy.

III.F Sub-Repository-Scale Models

Because it areally averages the thermal load, the repository-scale model cannot represent differences in temperature and saturation behavior within (1) the pillars, i.e., the rock separating neighboring emplacement drifts, (2) the emplacement drifts, or (3) the WPs themselves. The drift-scale model is a two-dimensional cross-sectional model that explicitly represents the details of the WPs and emplacement drifts in the plane orthogonal to the drift axes. This model is useful in representing details of thermo-hydrological behavior at the drift (or sub-repository) scale. We are interested in the detailed temperature distribution within and in the immediate vicinity of the emplacement drifts. We are also interested in how sub-repository-scale, buoyant, gas-phase convection, which is driven by temperature differences between the drifts and pillars, affects vapor and condensate flow and thermal performance.

To take advantage of symmetry, the drift-scale model assumes an infinite repository with uniformly spaced emplacement drifts. The assumption of an infinite repository area is applicable to the interior of the repository, which is not affected by cooling at the edge. This region includes most of the repository area during at least the first 1000 yr. The drift-scale model represents a symmetry element from the symmetry plane down the center of the WP to the symmetry plane in the pillar between neighboring drifts. The thermal load is axially averaged along the axis of the drift. The WP has a cross section of 1.6 × 1.6 m and is located in the center of an emplacement drift that is 4.8 m high by 6.0 m wide. This drift cross section is reasonably representative of a circular drift with a 7-m diameter. The drifts are assumed to remain open; therefore, heat flow from the WP surface to the drift wall occurs as thermal radiation, convection, and conduction. This model can represent heterogeneity that occurs at the scale of the drifts.

The drift-scale calculations apply the 21-PWR/40-BWR WP receipt scenario assumed in the repository-scale models with one important distinction. Rather than blending all of the WPs received over the 23-yr emplacement period, we assumed a WP receipt scenario which is more realistic. We blended the heat output for the first 63 21-PWR WPs and 46 40-BWR WPs received during the first two years of repository operation. Calculations were done for center-to-center drift spacings of 99, 66.8, 43.4, 28.8, and 21.7 m for AMLs of 24.2, 35.9, 55.3, 83.4, and 110.5 MTU/acre, respectively. In order to analyze the impact of sub-repository-scale, buoyant, gas-phase convection, we considered values of k_h of 10 and 280 millidarcy, and 168 darcy. For the 21-PWR and 40-BWR WP receipt scenario, a center-to-center WP spacing of 12 m was assumed. Note that these calculations are also applicable to a 12-PWR/21-BWR WP receipt scenario with a center-to-center WP spacing of 6.86 m.

IV. Discussion of Repository-Scale Model Results

IV.A Thermo-Hydrological Behavior

With the use of the repository-scale model, we modeled 26 cases, including 5 AMLs and 8 different values of bulk permeability, k_h. Table 1 summarizes the thermal performance at two locations in the repository for all 26 cases. All cases were modeled for a minimum of 100,000 yr. Rather than presenting the vertical temperature and saturation profiles for all 26 cases, we examine the profiles in detail for the suite of 280-millidarcy cases. In previous work,[4,8] we found that the threshold k_h where mountain-scale, buoyant, gas-phase convection begins to dominate moisture movement is about 1 darcy. Below this threshold, the effects of boiling tend to dominate the effects of buoyant, gas-phase convection. We chose to focus on the 280-millidarcy suite of cases, not because 280 millidarcy is considered to be the most likely value of k_h, but rather to more readily discern the impact of boiling behavior on moisture movement without the competing influence of mountain-scale, buoyant, gas-phase convection. A detailed examination of the impact of that convection on thermo-hydrological performance is presented in the following sections.

Figure 1 shows the temperature and saturation histories at various locations in the repository for the 110.5-, 83.4-, and 55.3-MTU/acre cases. Peak temperatures, T_{peak}, occur within the first 120 yr. In this report, we refer to radial location with respect to percentage of the repository area that it encloses. Therefore, a radial position of 0% corresponds to the repository center, while 100% corresponds to the outer perimeter. Notice that edge cooling effects do not penetrate to the inner 75% of the repository in the first 120 yr; consequently, T_{peak} is about the same for the inner 75% of the repository (Fig. 1a). For example, T_{peak} is 187.2°C at the repository center and 186.0°C at the 75% radial position. Edge cooling reduces T_{peak} for the outer 25% of the repository relative to the center. At the outer edge of the repository, T_{peak} is only 112.4°C. Edge cooling eventually penetrates into the center of the repository, reducing the duration of boiling, t_{hp}, even at the repository center.

Liquid saturation in the repository remains below ambient conditions long after boiling conditions have ceased for most of the repository. The inner 75% of the repository remains below ambient saturation for at least 100,000 yr (Fig. 1b). The inner 99% of the repository remains below ambient saturation for at least 10,000 yr, while the outer 1% re-wets nearly back to ambient saturation within 5000 yr.

The vertical temperature and saturation profiles are given for three different radial distances from the repository center (Figs. 2–4). The first value of r (r = 0 m) corresponds to the center of the repository. The second value of r corresponds to the radial position that encloses 50% of the repository. This position is representative of "average" conditions in the repository because half of the WPs are inside this radial position. The third value of r corresponds to the radial position that encloses 95% of the repository and is a good representation of conditions at the repository edge (or perimeter) because only 5% of the WPs lie outside of this position.

Figure 2 shows the vertical temperature and saturation profiles for the 110.5-MTU/acre case at various times after emplacement. Notice that the thermal and dry-out perfor-

mance is very similar for the 0 and 50% radial positions of the repository for the first thousand years and that edge cooling affects at least the outer 5% of the repository. The flattening of the temperature profile at the nominal boiling temperature, T_b (=96°C), corresponds to two-phase flow effects, which result from condensate drainage. These effects are described in more detail in other reports.[4-9] Dry-out due to boiling results in a 200- to 300-m-thick dry-out zone for the inner 50% of the repository. Edge cooling substantially reduces the vertical extent of dry-out. Temperatures at the outer edge of the repository drop below boiling at about 2000 yr (Fig. 1a), while the center remains above T_b for more than 7000 yr. Temperatures for the entire repository have declined to below T_b within 10,000 yr; however, a large zone of sub-ambient saturations persists long after that (Figs. 2b and c). The outer 5% of the repository rewets back to ambient saturation within 50,000 yr, while the center remains below ambient saturation for more than 100,000 yr (Fig. 1a).

The temperature and liquid saturation histories for the 83.4-MTU/acre case (Fig. 3) are similar to those of the 110.5-MTU/acre case, except that the duration of boiling and sub-ambient liquid saturation conditions is less (Figs. 1c and d). The inner 75% of the repository shows a similar T_{peak} (146°C). At the outer edge, T_{peak} is only 97.8°C.

Table I
Averaged thermal performance at two locations in the repository

Thermal loading conditions and bulk permeability, k_b				Center of repository				97% radial position in the repository			
AML (MTU/acre)	APD (kW/acre)	Area (acres)	k_b (darcy)	$T_{1000\ yr}$ (°C)	T_{peak} (°C)	t_{peak} (yr)	t_{bp} (yr)	$T_{1000\ yr}$ (°C)	T_{peak} (°C)	t_{peak} (yr)	t_{bp} (yr)
24.2	25	2598	0.28	62.9	65.7	145	NA	48.3	59.7	86	NA
24.2	25	2598	10	63.0	65.7	145	NA	47.9	59.7	86	NA
24.2	25	2598	40	63.1	65.7	145	NA	46.2	59.6	86	NA
24.2	25	2598	84	61.6	65.7	145	NA	42.2	59.3	86	NA
35.9	37	1755	0.28	81.6	85.8	143	NA	58.7	74.8	72	NA
35.9	37	1755	1	81.6	85.8	143	NA	58.6	74.8	72	NA
35.9	37	1755	10	82.0	85.9	143	NA	57.2	74.7	72	NA
35.9	37	1755	40	79.6	85.5	137	NA	50.3	74.0	72	NA
35.9	37	1755	84	77.2	84.9	140	NA	45.8	72.6	69	NA
55.3	57	1139	0.28	105.1	108.8	122	2152	73.1	96.7	61	85
55.3	57	1139	1	103.5	107.6	121	2092	73.1	96.4	60	60
55.3	57	1139	10	100.0	105.1	100	1471	69.4	93.7	50	0
55.3	57	1139	40	93.8	103.6	81	762	59.2	89.4	61	0
55.3	57	1139	84	89.4	102.3	80	403	54.7	86.8	50	0
83.4	86	755	0.28	139.3	146.0	181	5086	95.8	118.3	60	991
83.4	86	755	1	135.9	144.9	180	4811	92.8	117.4	61	814
83.4	86	755	10	128.0	134.6	121	4171	81.7	112.0	60	328
83.4	86	755	40	123.3	132.2	100	3724	73.8	110.4	60	189
83.4	86	755	84	119.6	130.4	100	2917	68.6	108.7	60	150
110.5	114	570	0.001	183.4	197.5	100	7988	116.4	153.2	60	2272
110.5	114	570	0.01	178.1	190.4	120	8091	114.0	148.1	60	2248
110.5	114	570	0.28	175.8	187.2	121	8105	112.4	144.0	60	2150
110.5	114	570	1	176.3	186.3	121	8125	108.7	142.0	60	1814
110.5	114	570	10	162.2	170.9	120	7997	97.1	131.6	50	1060
110.5	114	570	40	159.2	170.2	402	7743	89.2	132.3	61	721
110.5	114	570	84	156.5	169.8	202	6790	83.7	132.3	60	548

Most of the repository re-wets back to ambient saturation within 100,000 yr. Edge cooling causes the outer 1% of the repository to never undergo significant dry-out (Fig. 1d).

Figure 4 shows the vertical temperature and saturation profiles for the 55.3-MTU/acre case. Notice that the thermal and dry-out performance is similar to that of the 83.4-MTU/acre case except that the vertical extent of boiling and dry-out effects is substantially less. Moreover, the duration of boiling and sub-ambient liquid saturation conditions is substantially less for the 55.3-MTU/acre case

Figure 1. Temperature history (a) and liquid saturation history (b) at various repository locations relative to the repository center for an AML of 110.5 MTU/acre. Also plotted are temperature history (c) and liquid saturation history (d) for an AML of 83.4 MTU/acre, and temperature history (e) and liquid saturation history (f) for an AML of 55.3 MTU/acre. The locations are identified as the percentage of the repository area enclosed, with 0% corresponding to the repository center, and 100% corresponding to the outer perimeter of the repository. Note different temperature and time scales.

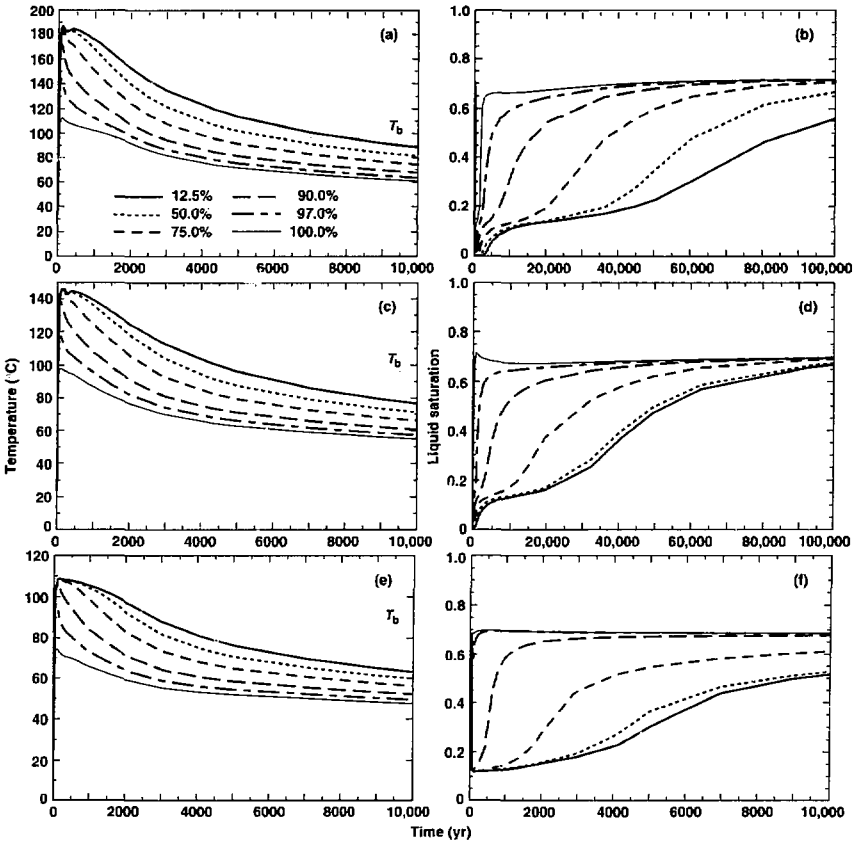

(Figs. 1e and f) than for the 83.4-MTU/acre case (Figs. 1c and d). Temperatures in the outer 3% of the repository never exceed T_b, and T_{peak} at the outer edge is only 74.7°C. Liquid saturations for the inner half of the repository re-wet back to ambient conditions in about 30,000 yr. Between the 50 and 75% radial positions, liquid saturations re-wet back to ambient conditions in about 20,000 yr. Re-wetting takes about 10,000 yr at the 84% radial position, 2000 yr at the 90% position, and 700 yr at the 94% position. At the 97% radial position, re-wetting takes about 150 yr, and dry-out never occurs for the outer 3% of the repository.

Figure 5 shows the temperature history for the 35.9- and 24.2-MTU/acre cases, respectively. Because of the large repository areas, cooling effects do not penetrate as far into the repository. Consequently, T_{peak} is about the same for the inner 90% of the repository (Figs. 5a and b). For the inner 50%, the entire temperature history is very similar. For the 35.9- and 24.2-MTU/acre cases, T_{peak} is 85.8 and 65.7°C, respectively.

Figure 2. Vertical temperature profiles at various radial distances, r, from the repository centerline for an AML of 110.5 MTU/acre at (a) t = 1000 yr, (b) t = 10,000 yr, and (c) t = 36,000 yr. Note different temperature scales. Vertical liquid saturation profiles are also plotted at (d) t = 1000 yr, (e) t = 10,000 yr, and (f) t = 36,000 yr.

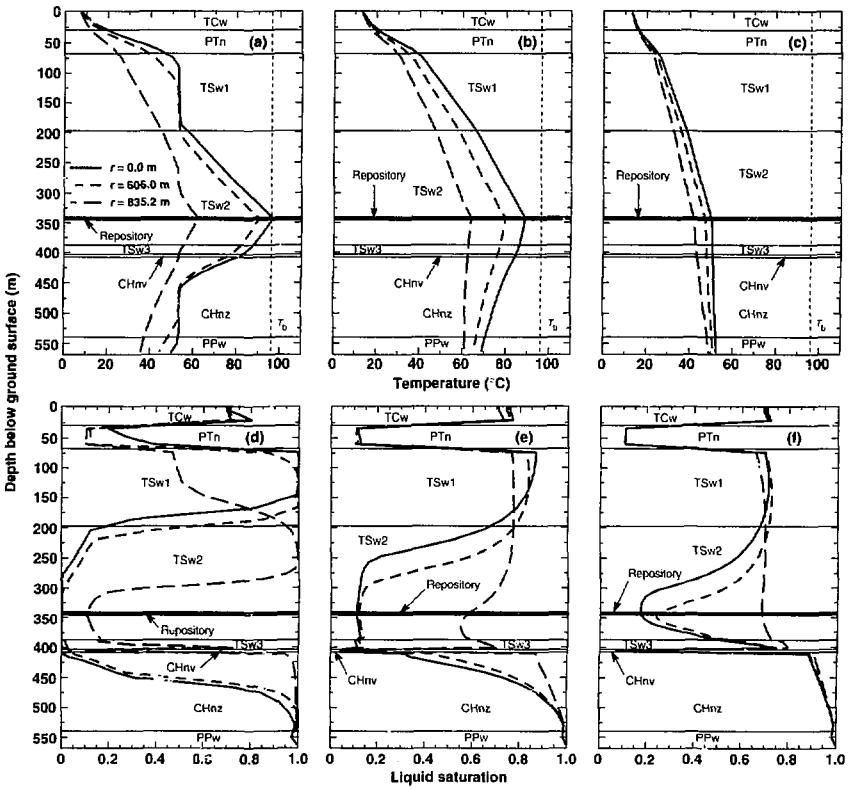

Edge cooling reduces T_{peak} for the outer 10% of the repository relative to the center. At the outer edge, T_{peak} is 58.2 and 47.8°C for the 35.9- and 24.2-MTU/acre cases, respectively.

Figure 6 shows the vertical temperature profiles for the 35.9- and 24.2-MTU/acre cases. Notice that the repository-scale model does not predict temperatures to exceed T_b, indicating that averaged temperature conditions throughout the repository remain below boiling. However, as will be discussed later, local temperatures around the emplacement drift may be well above boiling for WPs containing a large number of SNF assemblies. Because of the absence of boiling conditions in the repository-scale model, and because 280 millidarcy is below the threshold where mountain-scale, buoyant, gas-phase convection results in significant moisture movement, the 24.2- and 35.9-MTU/acre cases show a minor change in saturation relative to ambient conditions. Therefore, we did not provide the vertical saturation profiles for these two cases.

Figure 3. Vertical temperature profiles at various radial distances, r, from the repository centerline for an AML of 33.4 MTU/acre at (a) t = 1000 yr, (b) t = 10,000 yr, and (c) t = 33,000 yr. Note different temperature scales. Vertical liquid saturation profiles are also plotted at (d) t = 1000 yr, (e) t = 10,000 yr, and (f) t = 33,000 yr.

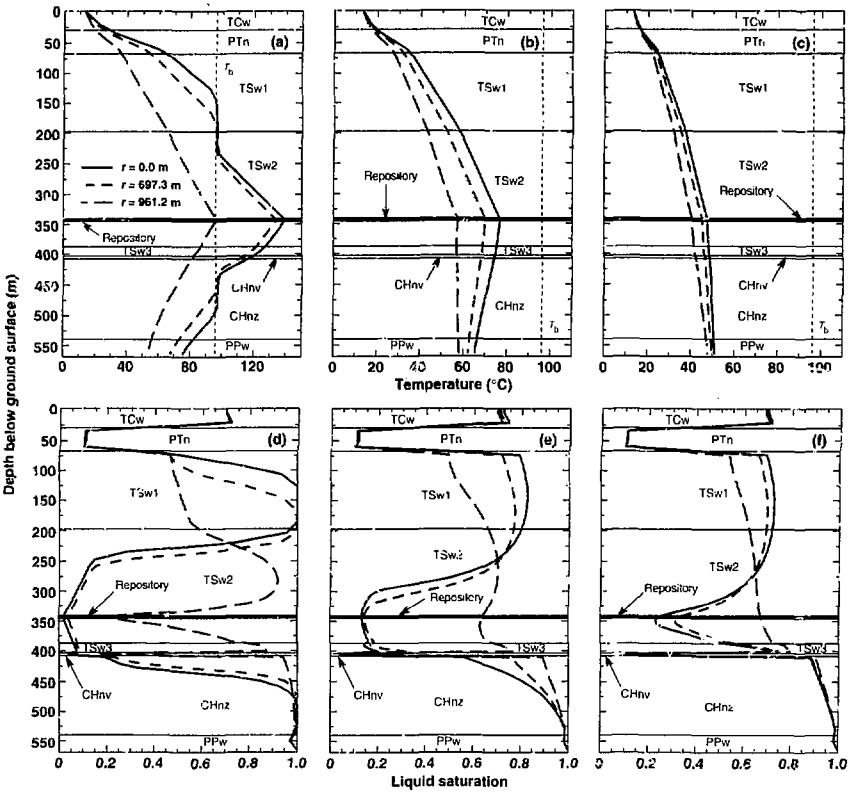

As in past studies,[7,8] when analyzing dry-out and re-wetting behavior, we use the term, normalized liquid saturation, $\overline{S}_l$, which is given by

$$\overline{S}_l = \frac{S_l}{S_{l,\text{init}}} \tag{4}$$

where S_l is the current liquid saturation and $S_{l,\text{init}}$ is the initial (or ambient) liquid saturation. To compare the re-wetting behavior of various AMLs, we compared the duration of time that S_l in the repository is below 90% of ambient (Fig. 7) as a function of repository location. Because $\overline{S}_l = 0.9$ when S_l has been restored to 90% of ambient, we call this time $t(\overline{S}_l = 0.9)$. For the inner 12.5% of the repository, $t(\overline{S}_l = 0.9)$ is 118,413 and 77,290 yr for 110.5 and 83.4 MTU/acre, respectively. For the inner 50% of the 55.3-MTU/acre repository, $t(\overline{S}_l = 0.9)$ is 22,150 yr.

Edge cooling substantially reduces $t(\overline{S}_l = 0.9)$ for the outer repository area (Fig. 7). The impact of edge cooling on $t(\overline{S}_l = 0.9)$ at the repository edge increases

Figure 4. Vertical temperature profiles at various radial distances, r, from the repository centerline for an AML of 55.3 MTU/acre at (a) t = 1000 yr, (b) t = 10,000 yr, and (c) t = 36,000 yr. Vertical liquid saturation profiles are also plotted at (d) t = 1000 yr, (e) t = 10,000 yr, and (f) t = 36,000 yr.

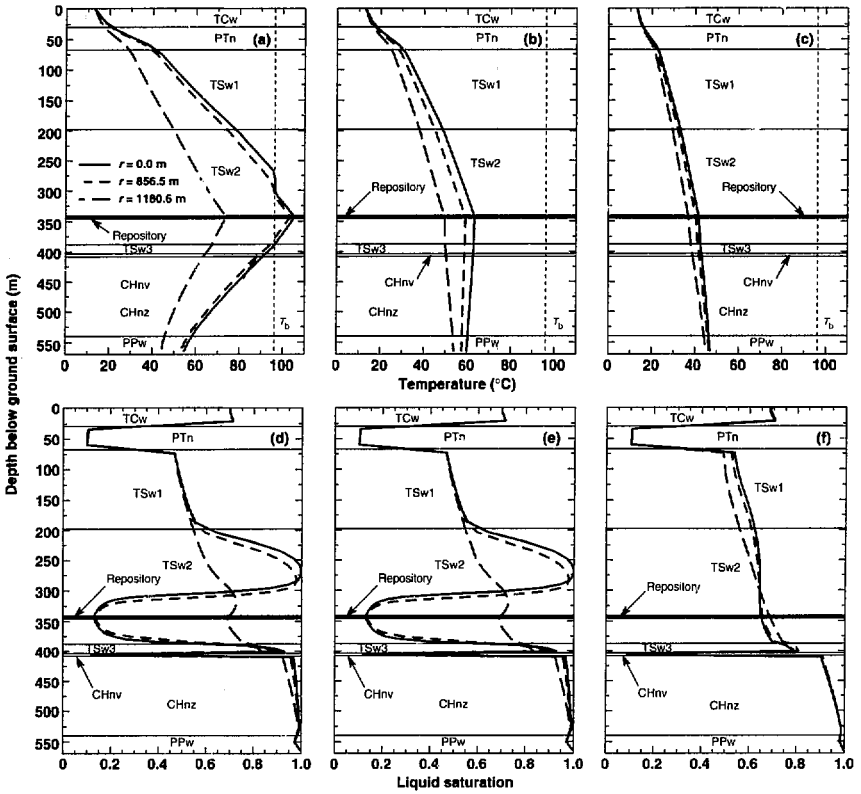

with decreasing AML. At the 90% repository location, $t(\bar{S}_l = 0.9)$ is 30,339, 20,442, and 1172 yr for AMLs of 110.5, 83.4, and 55.3 MTU/acre, respectively. For 55.3 MTU/acre, dry-out never occurs for the outer 3% of the repository. At the outer edge (100% repository location), $t(\bar{S}_l = 0.9)$ is 1996 and 289 yr for 110.5 and 83.4 MTU/acre, respectively. We also calculated the area-weighted $t(\bar{S}_l = 0.9)$, which we call $\bar{t}(\bar{S}_l = 0.9)$. This is effectively equivalent to $t(\bar{S}_l = 0.9)$ for an "average" WP in the repository. For AMLs of 110.5, 83.4, and 55.3 MTU/acre, $t(\bar{S}_l = 0.9)$ is 71,712, 57,414, and 14,929 yr, respectively.

Figure 8 shows the duration of the boiling period, t_{bp}, as a function of radial position for the 110.5-, 83.4-, and 55.3-MTU/acre cases and all of the values of k_h considered. The influence of edge cooling is evident. Notice the effect that increasing k_h has on decreasing t_{bp}. Mountain-scale, buoyant, gas-phase convection begins to significantly cool repository temperatures for $k_h > 1$ darcy. For $k_h \leq 1$ darcy, $\bar{t}_{bp}$ is insensitive to k_h.

Figure 5. Temperature history at various repository locations for an AML of (a) 35.9 MTU/acre, and (b) 24.2 MTU/acre. The locations are identified as the percentage of the repository area enclosed, with 0% corresponding to the repository center, and 100% corresponding to the outer perimeter.

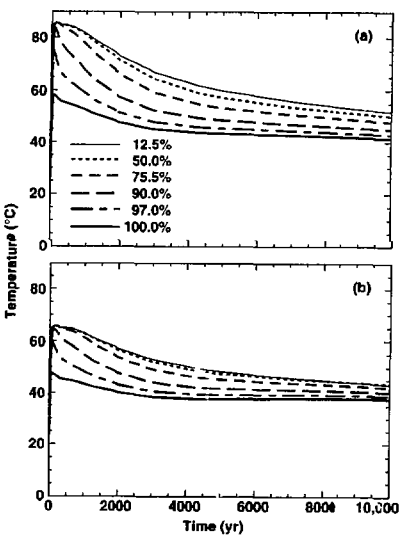

Notice that the sensitivity of t_{bp} to k_h increases with decreasing AML.

Figure 9 shows the area-weighted boiling period duration, $\bar{t}_{bp}$, for various k_h values as a function of AML. For the 280-millidarcy cases, $\bar{t}_{bp}$ is 5446, 3391, and 1424 yr for AMLs of 110.5, 83.4, and 55.3 MTU/acre, respectively. The cooling effect that mountain-scale, buoyant, gas-phase convection has on $\bar{t}_{bp}$ increases with decreasing AML. Accordingly, the 110.5-MTU/acre case is least sensitive to this effect. For the 110.5-MTU/acre, 1-darcy case, this cooling effect reduces $\bar{t}_{bp}$ by 2.9% relative to the 280-millidarcy case, while for 83.4 and 55.3 MTU/acre, $\bar{t}_{bp}$ is reduced by 8.3 and 4.3%, respectively. For the 110.5-MTU/acre, 10-darcy case, $\bar{t}_{bp}$ is reduced by 17.5% relative to the 280-millidarcy case, while for 83.4 and 55.3 MTU/acre, the reduction is 29.2 and 34.9%, respectively. For the 110.5-MTU/acre, 40-darcy case, $\bar{t}_{bp}$ is reduced by 28.6% relative to the 280-millidarcy case, while for 83.4 and 55.3 MTU/acre, the reduction is 39.4 and 73.7%, respectively. For the 110.5-MTU/acre, 84-darcy case, $\bar{t}_{bp}$ is reduced by 40.7% relative to the 280-millidarcy case, while for 83.4 and 55.3 MTU/acre, the reduction is 53.1 and 88.5%, respectively.

IV.B Mountain-Scale Moisture Redistribution

We compared the net buildup of liquid water above the repository, ΔV_l, for all of the thermal loads and k_h cases (Fig. 9). For the high-k_h, high-AML cases (10, 40, and 84 darcy; 83.4 and 110.5 MTU/acre), a very early peak in ΔV_l occurs at 500 to 800 yr (Figs. 9c–e), coinciding with the maximum extent of boiling conditions. After the initial peak, ΔV_l declines for the high-k_h, high-AML cases, with a trough occurring at 3000 yr, coinciding with the maximum vertical extent of dry-out. For 110.5 MTU/acre, ΔV_l declines to below zero (Figs. 9d and e). For 83.4 MTU/acre, the trough is less pronounced as ΔV_l stays well above zero (Figs. 9c–e). After the trough occurs in the 83.4- and 110.5-MTU/acre cases, the increase in ΔV_l resumes until a second peak in ΔV_l occurs at around 20,000 to 30,000 yr. For the 55.3-MTU/acre case, there is no trough, and the increase in ΔV_l is uninterrupted (Figs. 9a–e). For 10, 40, and 84 darcy, the 55.3-, 83.4-, and 110.5-MTU/acre cases undergo the same initial rate of increase in ΔV_l until 500 yr, when the 110.5-MTU/acre case reaches its initial peak, and 800 yr, when the 83.4-MTU/acre case reaches its initial peak (Figs. 10c–e). This initial peak is related to the interaction of the heat-pipe effect and mountain-scale, buoyant, gas-phase convection.

It is important to note that ΔV_l is always greater in the 55.3- and 83.4-MTU/acre cases than in the 110-MTU/acre case. We plot the maximum ΔV_l (called ΔV_l^{max}) for all of the AMLs and values of k_h considered

(Fig. 9f). For 55.3 MTU/acre, ΔV_l^{max} is 1.5, 1.3, 2.4, 2.6, and 2.5 times greater than in the 110.5-MTU/acre case for 280 millidarcy and 1, 10, 40, and 84 darcy, respectively. For 83.4 MTU/acre, ΔV_l^{max} is 1.5, 1.7, 1.4, 1.4, and 1.5 times greater than in the 110.5-MTU/acre case for 280 millidarcy and 1, 10, 40, and 84 darcy, respectively. To the first order, for intermediate to high AMLs, ΔV_l^{max} is proportional to the repository area. For the 110.5-MTU/acre case and $k_h < 10$ millidarcy, ΔV_l is always negative (i.e., there is a net decrease in liquid saturation). Consequently, if the large-scale connected k_h is small enough, mountain-scale, buoyant, gas-phase convection does not result in a liquid water buildup above the repository.

For 280 millidarcy, ΔV_l^{max} for 24.4 and 35.9 MTU/acre is 26 and 34% of ΔV_l^{max} for the 110.5-MTU/acre case; however, ΔV_l^{max} for the latter case is relatively small to begin with. For 10 darcy, ΔV_l^{max} for 24.4 and 35.9 MTU/acre is 50 and 105% of ΔV_l^{max} for the 110.5-MTU/acre case. For 40 darcy, ΔV_l^{max} for 24.4 and 35.9 MTU/acre is 1.7 and 2.9 times greater than in the 110.5-MTU/acre case. For 84 darcy, ΔV_l^{max}

Figure 6. Vertical temperature profiles at various radial distances, r, from the repository centerline for an AML of 35.9 MTU/ acre at (a) t = 1000 yr, (b) t = 10,000 yr, and (c) t = 32,000 yr. Vertical temperature profiles for an AML of 24.2 MTU/acre are also plotted at (d) t = 1000 yr, (e) t = 10,000 yr, and (f) t = 30,000 yr. Note different temperature scales.

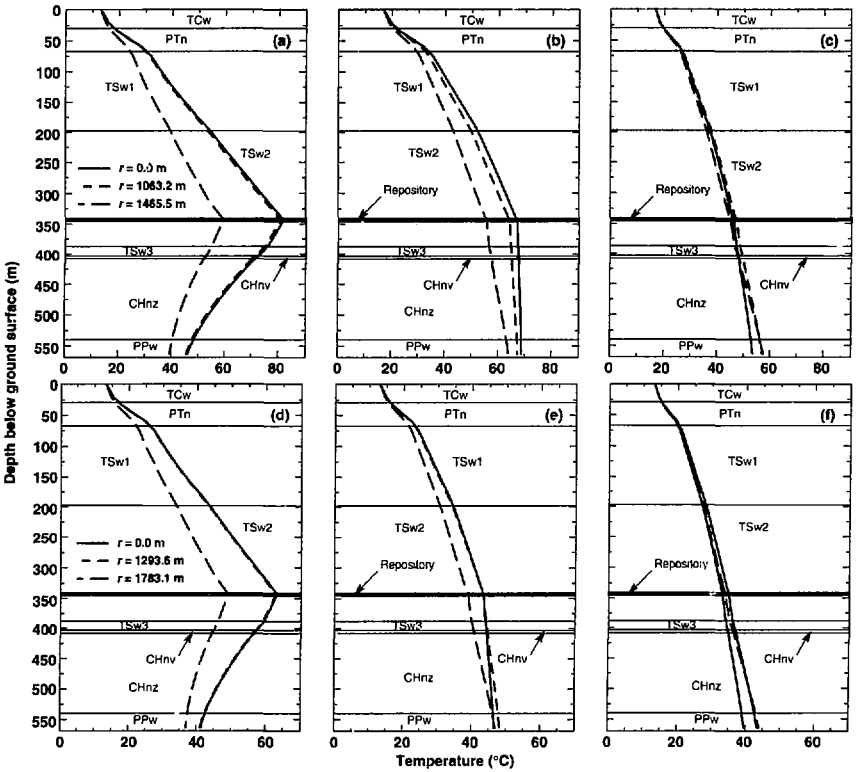

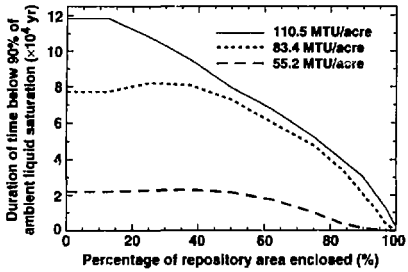

Figure 7. Duration of time during which liquid saturation at various repository locations is below 90% of the ambient value, for k_h = 280 millidarcy and various AMLs. The locations are identified as the percentage of the repository area enclosed, with 0% corresponding to the repository center, and 100% corresponding to the outer perimeter.

for 24.4 and 35.9 MTU/acre is 2.8 and 3.4 times greater than in the 110.5-MTU/acre case. Therefore, for low k_h (k_h < 1 darcy), the low-AML cases result in less net liquid water buildup than the high-AML cases, while for high k_h (k_h > 40 darcy), ΔV_l^{max} is proportional to the repository area.

It is important to note that because the ECM cannot represent nonequilibrium fracture-matrix flow, it underpredicts the condensate drainage flux and, consequently, overpredicts ΔV_l. However, ΔV_l is a useful indicator (or surrogate) of the overall magnitude of condensate drainage flux and saturation buildup effects. The slope of the ΔV_l vs t curve is indicative of the overall rate of condensate generation that arises from mountain-scale, buoyant vapor flow. For high AMLs, it is indicative of the competition between vapor flow driven by the gas-pressure buildup due to boiling, and vapor flow driven by thermal buoyancy.

It is also important to point out that the purpose of this study is to illustrate the general sensitivity of large-scale thermo-hydrological behavior to a wide range of

Figure 8. Duration of the boiling period at various repository locations for AMLs of (a) 110.5, (b) 83.4, and (c) 55.3 MTU/acre. The locations are identified as the percentage of the repository area enclosed, with 0% corresponding to the repository center, and 100% corresponding to the outer perimeter. (d) Area-weighted duration of the boiling period as a function of AML.

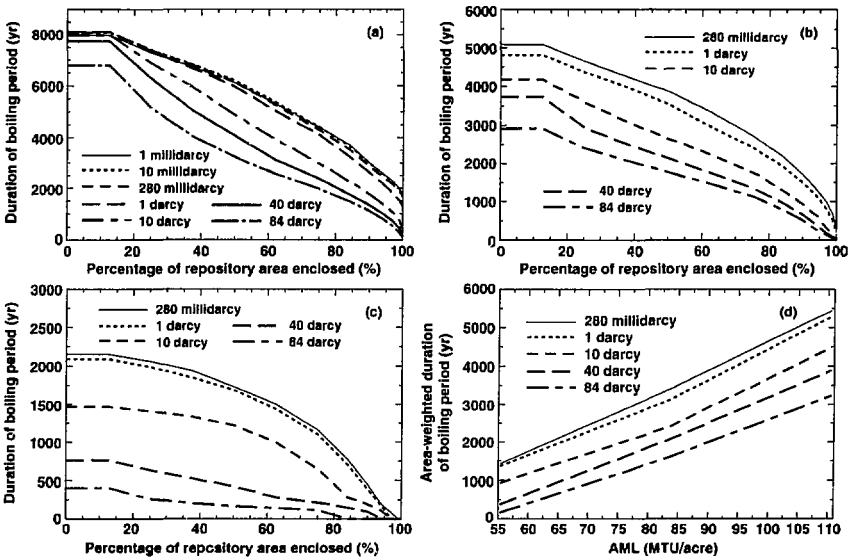

conditions through the use of macroscopic parameters such as t_{bp}, ΔV_l, and ΔV_l^{max}. Any attempt to make specific inferences of this behavior on waste package performance and radionuclide transport would require a far more detailed look at the spatial distribution of the repository-heat-driven changes to temperatures, liquid saturations, and vapor and liquid fluxes than can be addressed in this report.

It is likely that the k_h distribution at Yucca Mountain will be highly variable. Some of that variability will be random, while some may be correlated with discrete hydrological features like fault zones or hydrostratigraphic units such as the nonwelded vitric tuff units (PTn and CHnv). According to Weeks,[16,17] in at least some portions of the repository horizon in the TSw2, k_h may be on the

Figure 9. Net buildup of liquid water above the repository vs time for various AMLs and k_h values of (a) 280 millidarcy and (b) 1, (c) 10, (d) 40, and (e) 84 darcy. (f) Maximum net buildup of liquid water above the repository as a function of AML for various values of k_h.

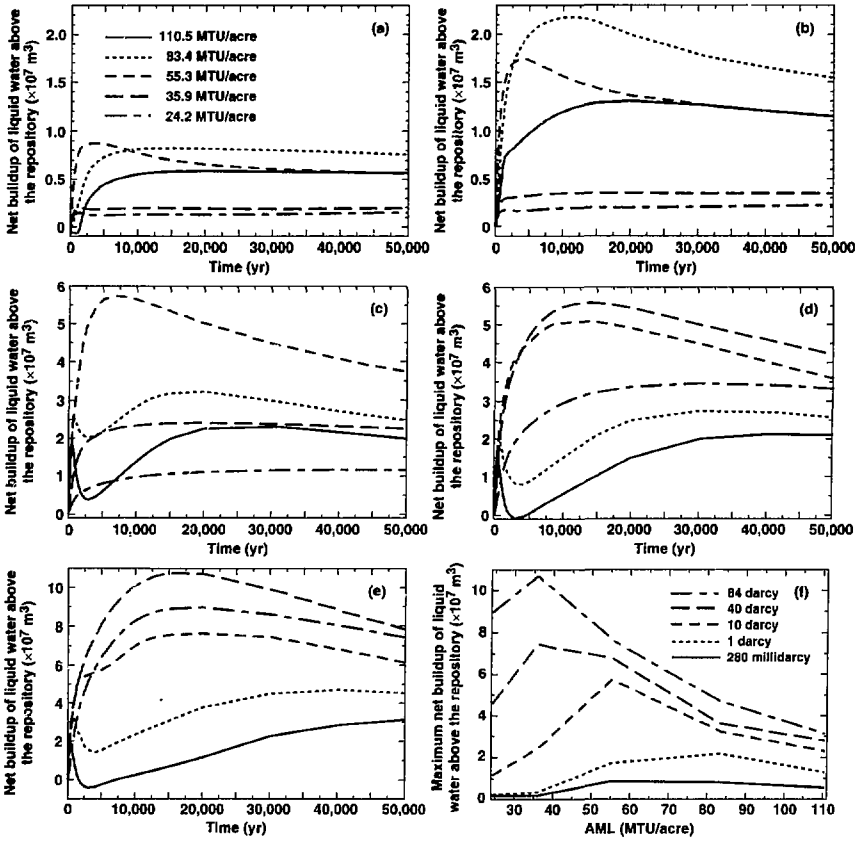

order of 200 darcy, while in other units such as the PTn, CHnv, and CHnz, it is much smaller (k_h < 1 darcy). As in other studies,[4,8,9] this study considered a very wide range of k_h in order to identify where distinct changes in thermo-hydrological behavior occur. These sensitivity analyses are needed to assist in the development of a robust site characterization and testing program that will obtain the requisite data for establishing repository performance.

It should be pointed out that this sensitivity study of mountain-scale moisture movement was done for the idealized situation of a uniform k_h distribution. Ref. 9 considers the situation in which the k_h distribution varies vertically, which results in a layered heterogeneous k_h distribution. That study found that a reduction in k_h over relatively narrow depth intervals can substantially influence mountain-scale moisture movement.

V. Discussion of Sub-Repository-Scale Model Results

V.A Temperature History in the Vicinity of the Emplacement Drift

The preceding analysis represents averaged thermo-hydrological behavior in the repository. To investigate the details of behavior in the vicinity of WPs, it is necessary to use sub-repository-scale (or drift-scale) models. Using the drift-scale model, we conducted calculations for AMLs of 24.2, 35.9, 55.3, 83.4, and 110.5 MTU/acre. In order to analyze the impact of sub-repository-scale, buoyant, gas-phase convection, we considered values of k_h of 10 and 280 millidarcy, and 168 darcy. Table II summarizes the thermal performance on the waste package (WP) surface and in the rock 0.75 m above the drift ceiling for all of the cases considered. Our earlier drift-scale calculations,[3] which blended 23 yr of WPs received by the repository, resulted in peak WP temperatures occurring at t_{peak} = 125 yr. In those calculations, the heat output from an individual WP is ramped up in the same fashion as in the repository-scale model rather than being instantaneously raised to the full-power equivalent of an individual WP. Using the WP receipt schedule that more realistically accounts for local heating conditions, the drift-scale models in this study predict 12 < t_{peak} < 70 yr (Table II).

A critical issue to address in analyzing the thermo-hydrological performance in the vicinity of the emplacement drifts is the potential for sub-repository-scale, buoyant, gas-phase convection, which can occur within fracture networks having a connectivity with

Table II
Thermal performance for 21-PWR WPs and 40-BWR WPs with 12-m center-to-center spacing between WPs; also applicable to 12-PWR WPs and 21-BWR WPs with 6.86-m center-to-center WP spacing

Thermal loading conditions and bulk permeability, k_h				Waste package surface				0.75 m above the drift ceiling in the rock			
AML (MTU/acre)	APD (kW/acre)	Drift spacing (m)	k_h (darcy)	$T_{1000\,yr}$ (°C)	T_{peak} (°C)	t_{peak} (yr)	t_{bp} (yr)	$T_{1000\,yr}$ (°C)	T_{peak} (°C)	t_{peak} (yr)	t_{bp} (yr)
24.2	25	99.0	0.01	80.0	171.8	12.6	350	76.2	144.1	14.4	202
24.2	25	99.0	0.28	79.4	170.4	12.8	310	75.8	142.2	17.6	195
24.2	25	99.0	168	79.0	164.0	12.5	300	75.4	133.0	14.5	183
35.9	37	66.8	0.01	99.3	172.5	14.1	1155	96.3	146.1	19.3	1014
35.9	37	66.8	0.28	99.2	170.7	12.4	1148	96.2	144.4	25.2	1010
35.9	37	66.8	168	97.7	165.2	12.8	1111	94.9	135.4	19.0	955
55.3	57	43.4	0.01	125.3	184.6	25.1	2438	123.0	165.5	35.3	2379
55.3	57	43.4	0.28	120.5	181.6	20.0	2394	118.0	160.7	25.0	2316
55.3	57	43.4	168	120.1	169.0	14.3	2029	117.7	136.8	18.1	1828
83.4	86	28.8	0.01	162.6	219.9	50.0	3964	160.9	208.8	60.1	3885
83.4	86	28.8	0.28	157.2	202.0	40.1	3966	155.4	188.0	45.8	3873
83.4	86	28.8	168	154.0	169.0	40.0	3415	152.1	182.8	60.3	3338
110.5	114	21.7	0.01	203.3	269.9	60.0	5725	201.9	262.7	60.0	5594
110.5	114	21.7	0.28	192.5	247.5	50.2	5574	190.9	238.2	60.7	5430
110.5	114	21.7	168	188.1	242.2	60.0	5548	186.4	233.6	70.4	5408

length scale comparable to the distance between the hot and cold regions of the repository. Buoyant, gas-phase convection cells develop as the warmer, less-dense column of gas within the footprint of the WPs is displaced by the cooler, denser column of gas in the adjacent areas. As the initially cooler gas is heated up, its relative humidity is lowered, causing it to evaporate water from the rock matrix below hot regions of the repository. This warm moist air is convected upward to where it cools above the WPs, generating condensate that drains down fractures back toward the repository and/or is imbibed by the matrix, causing a saturation buildup above the WPs.

High AMLs result in a large zone of above-boiling temperatures that suppresses the effects of repository-scale, buoyant vapor flow.[4,9] Sub-repository-scale, buoyant, gas-phase convection continues as long as significant temperature differences persist within the repository. It can dominate moisture movement for up to 1000 yr for the drift spacing described in the Site Characterization Plan–Conceptual Design Report (SCP–CDR).[4,18] The larger drift spacing that is consistent with the use of larger WPs will result in temperature differences within the repository persisting longer. Consequently, the effects of sub-repository-scale, buoyant vapor flow will also be more persistent, possibly lasting thousands of years. In previous work,[4] we found that the threshold k_b where sub-repository-scale, buoyant vapor flow begins to dominate moisture movement is about 1 darcy. If, as Weeks[16] suggests, k_b at the repository horizon is found to be on the order of 200 darcy, the impact of sub-repository-scale, buoyant, gas-phase convection will be extremely significant.

The most important observation about sub-repository-scale performance concerns the substantial difference between thermal performance predicted by repository-scale models and that predicted by drift-scale models. For an AML of 24.2 MTU/acre, the repository-scale models predict a peak temperature, T_{peak}, of 65°C, while the drift-scale models predict T_{peak} of up to 171.8°C on the WP surface and 144.1°C in the rock adjacent to the drift. While the repository-scale model predicts no boiling period (Fig. 5b), the drift-scale model predicts a boiling period duration, t_{bp}, of 183 to 202 yr in the rock and from 300 to 350 yr on the WP surface (Table II). Similarly, the repository-scale model predicts no boiling period for an AML of 35.9 MTU/acre (Fig. 5a). However, the drift-scale model predicts t_{bp} of 955 to 1014 yr in the rock and 1111 to 1155 yr on the WP surface (Table II).

Another important observation about sub-repository-scale performance is that T_{peak} varies modestly for AMLs ranging from 24.2 to 55.3 MTU/acre (Figs. 10a and b). Because it occurs so early (12 to 25 yr), T_{peak} is relatively insensitive to whether the distance to the adjacent emplacement drift is 43.4 m or 99.0 m. For the high AMLs, the drift spacing is small enough to cause T_{peak} to be sensitive to center-to-center drift spacing. Consequently, T_{peak} is significantly greater for the 110.5-MTU/acre case than for the 83.4-MTU/acre case (Figs. 10a and b).

V.B Sub-Repository-Scale Moisture Redistribution

Figure 11 plots the dimensionless liquid saturation distribution orthogonal to an emplacement drift containing either (1) 21-PWR and 40-BWR WPs with a 12-m center-to-center spacing between WPs, or (2) 12-PWR and 21-BWR WPs with 6.86-m spacing between WPs. The center-to-center drift spacing is 99 m, yielding an AML of 24.2 MTU/acre. Figure 11 is plotted at 300 yr, which is about the end of the boiling period for the WP surface. For the uniform 10-millidarcy case, boiling has resulted in a small dry-out zone surrounding the emplacement drift (Fig. 11a), while for the uniform 168-darcy case, the dry-out zone is considerably larger (Fig. 11c). The difference in dry-out volume between these two cases

Figure 10. Temperature history (a) on the WP surface, and (b) in the rock 0.75 m above the center of the drift ceiling for k_b = 280 millidarcy and various AMLs. The heating curve is a composite for 46 40-BWR WPs and 63 21-PWR WPs received during the first two years of repository operation.

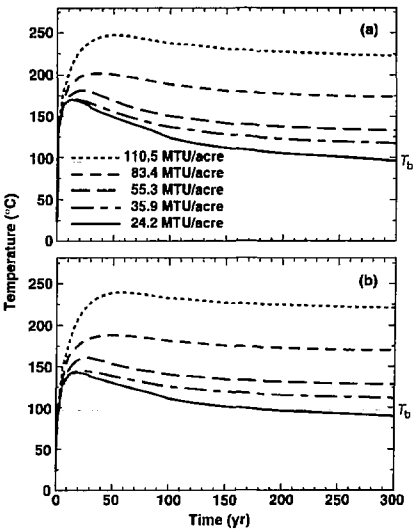

can be attributed to the influence of sub-repository-scale, buoyant, gas-phase convection. Buoyant convection is also responsible for driving all of the condensate buildup above the drift (Fig. 11c). Buoyant convection continues to drive significant vapor and condensate flow for about 2000 yr (long after boiling conditions have ceased).

Many of our calculations[6-8] have assumed a homogeneous k_h distribution and therefore do not address how heterogeneity might cause focused vapor and condensate flow. In Fig. 11b we use a highly idealized example to illustrate how heterogeneity at the sub-repository-scale might result in focused vapor and condensate flow in the vicinity of an emplacement drift. In this example, a 1.6-m-wide, high-k_h zone is aligned along the axis of the WP and flanked by low-k_h zones. The gas-phase pressure differential between these zones drives water vapor back toward the drift and into the high-k_h zone. Water vapor flows up the high-k_h zone until it condenses and drains back down. Enough water vapor enters and condenses in this zone to cause the condensate drainage flux to be large enough to maintain refluxing in the repository. The resulting heat-pipe effect enables the temperature at the top of the drift to remain at the nominal boiling point for the entire duration of the boiling period (about 300 yr), causing a depression in the dry-out zone. This refluxing zone persists for more than 2000 yr, long after boiling has ceased. This example is similar to calculations conducted in a previous study,[4] where we showed that spatial variability of hydrological properties can strongly influence thermo-hydrological behavior under sub-boiling conditions. We applied the same three k_h distributions shown in Fig. 11 to AMLs of 24.2, 35.9, 55.3, 83.4, and 110.5 MTU/acre. For the 83.4- and 110.5-MTU/acre cases, the thermo-hydrological behavior was virtually the same for the three different k_h distributions.

In general, we found that t_{hp} is insensitive to sub-repository-scale, buoyant, gas-phase convection for the low- and high-AML cases (24.2, 35.9, and 110.5 MTU/acre). For the intermediate-AML cases (55.3 and 83.4 MTU/acre), t_{hp} is modestly sensitive to sub-repository-scale, buoyant, gas-phase convection. For the high-AML cases, the extent

Figure 11. Dimensionless liquid saturation distribution orthogonal to an emplacement drift for an AML of 24.2 MTU/acre at t = 300 yr. The heating curve is a composite for 46 40-BWR WPs and 63 21-PWR WPs received during the first two years of repository operation. Dimensionless liquid saturation distributions are shown for (a) a uniform k_h of 10 millidarcy, (b) a heterogeneous k_h distribution consisting of alternating 1.6-m-wide, 168-darcy, high-k_h zones and 97.4-m-wide, 10-millidarcy zones, and (c) a uniform k_h of 168 darcy. The medium-shaded area surrounding the drift corresponds to a region that is drier than ambient saturation (dry-out zone). The dark-shaded areas correspond to regions that are wetter than ambient saturation (condensation zones). The lighter shading surrounding the dark-shaded areas corresponds to a decreasing buildup in saturation (outer edges of condensation zones). No shading indicates no change in saturation.

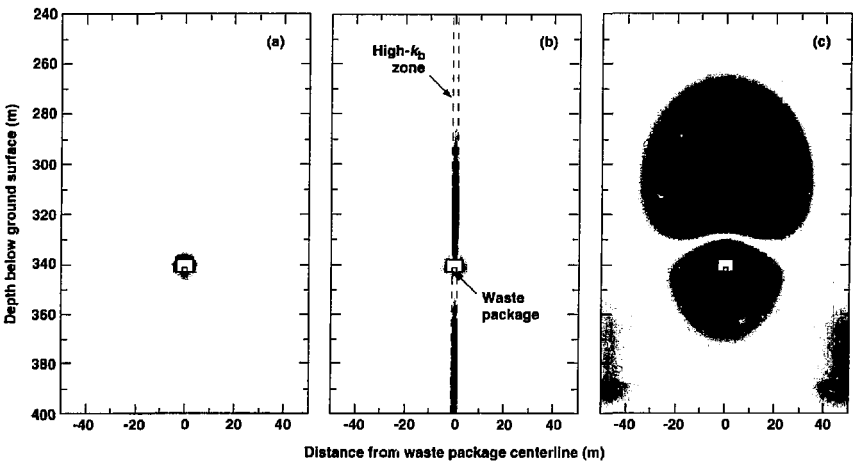

of dry-out is insensitive to sub-repository-scale, buoyant, gas-phase convection. For the low-AML cases, the extent of moisture movement (i.e., dry-out and condensate buildup) is extremely dependent on the magnitude of sub-repository-scale, buoyant, gas-phase convection.

There has been considerable debate over what constitutes a "cold" repository. One view is that a "cold" repository is one in which local temperatures never exceed boiling. Another view is that it is only necessary for the average repository temperature never to exceed boiling. What is not usually stated, but sometimes implied, is that sub-boiling temperatures can be equated with the absence of significant repository-heat-driven effects. Our analyses show that boiling conditions can persist around an emplacement drift even if the average repository temperature is well below the boiling point. Moreover, if buoyant, gas-phase convection is found to be significant, it can drive substantial vapor and condensate fluxes whether or not boiling occurs. On the other hand, if buoyant, gas-phase convection is found to be insignificant, a boiling period of sufficiently limited duration may be shown to generate condensate fluxes that have a minor impact on performance. However, the absence of local boiling conditions is not, in itself, an adequate indicator of whether repository heat drives significant vapor and condensate flow. Average repository temperatures are an even poorer indicator of the significance of repository-heat-driven hydrothermal flow in the performance of a low-AML repository. Diagnosing whether sub-boiling conditions can be equated with the absence of significant repository-heat-driven effects will require *in situ* heater tests conducted under sub-boiling as well as above-boiling conditions.[19,20]

VI. Conclusions

The radioactive heat-of-decay from spent nuclear fuel will play a dominant role in the performance of a potential repository at Yucca Mountain. Coupled hydrothermal-geochemical processes can strongly affect the composition and flow rates of gas and liquid around the waste packages. Waste package degradation, waste-form dissolution, and radionuclide release will critically depend on these processes. Repository heat will also play a dominant role in the evolution of the flow field that will drive gas-phase and liquid-phase transport. In addition, coupled hydrothermal-geochemical phenomena may significantly affect the performance of natural barriers underlying the repository. Depending on the thermal-loading management strategy (which will affect the design and operation of the repository) and site conditions, repository heat may either substantially increase the likelihood of water contacting waste packages and the magnitude of release and transport of radionuclides or preclude, or at least minimize, these effects for some period of time.

In our modeling studies, our approach has been to identify conditions that could potentially generate adverse performance. Accordingly, we have considered a wide range of bulk permeability values and examples of heterogeneity that may be extreme. This work provides a context for understanding the relative importance of various hydrogeological properties and features that will be determined during site characterization. This work also shows that the challenge of adequately understanding repository-heat-driven vapor and condensate flow is at least as formidable for sub-boiling conditions as it is for above-boiling conditions. Long-term *in situ* heater tests, conducted under both sub-boiling and above-boiling conditions, are required to determine the potential for the major repository-heat-driven sources of fracture flow to impact waste package performance and radionuclide transport.

Acknowledgments

The authors acknowledge the helpful comments of Jim Blink during the past year and the review of Bill Halsey. We acknowledge the very powerful post-processing software developed by Stephanie Daveler. We also appreciate the assistance of Rick Wooten, who prepared the graphics, and the editorial assistance of Jay Cherniak. We also thank Marion Capobianco for assisting in the text layout. This work was supported by the Near-field Hydrology Task (WBS 1.2.1.5) of the Yucca Mountain Site Characterization Project. Work performed under the auspices of the U.S. Department of Energy by Lawrence Livermore National Laboratory under Contract W-7405-Eng-48.

References

1. Montazer, P., and W.E. Wilson, "Conceptual Hydrologic Model of Flow in the Unsaturated Zone, Yucca Mountain, Nevada," Water Resources Investigation Report 84-4345, U.S. Geological Survey (1984).

2. Klavetter, E.A., and R.R. Peters, "Estimation of Hydrologic Properties of an Unsaturated Fractured Rock Mass," *SAND84-2642*, Sandia National Laboratories, Albuquerque, NM (1986).

3. Saterlie, S.F., and B. Thompson, "FY93 Thermal Loading Systems Study Final Report, Volume 1," prepared by Civilian Radioactive Waste Management System Management and Operating Contractor, TRW Environmental Safety Systems, Inc., Las Vegas, NV, December 30, 1993.

4. Buscheck, T.A., and J.J. Nitao, "The Impact of Repository Heat on Thermo-Hydrological Performance at Yucca Mountain," *Proceedings American Nuclear Society Topical Meeting on Site Characterization and Model Validation (Focus 93)*, Las Vegas, NV, Sept. 26–30, 1993.

5. Pruess, K., and Y.W. Tsang, "Modeling of Strongly Heat-Driven Processes at a Potential High-Level Nuclear Waste Repository at Yucca Mountain, Nevada," *Proceedings Fourth International High-Level Radioactive Waste Management Conference*, Las Vegas, NV, April, 1993.

6. Buscheck, T.A., and J.J. Nitao, "The Impact of Thermal Loading on Repository Performance at Yucca Mountain," American Nuclear Society, *Proceedings Third International High-Level Radioactive Waste Management Conference*, Las Vegas, NV, April 12–16, 1992. Also, *UCRL-JC-109232*, Lawrence Livermore National Laboratory, Livermore, CA (1992).

7. Buscheck, T.A., and J.J. Nitao, "The Impact of Repository-Heat-Driven Hydrothermal Flow on Hydrological Performance at Yucca Mountain," American Nuclear Society, *Proceedings Fourth International High-Level Radioactive Waste Management Conference*, Las Vegas, NV, April 1993. Also, *UCRL-JC-112444*, Lawrence Livermore National Laboratory, Livermore, CA (1993).

8. Buscheck, T.A., and J.J. Nitao, "Repository-Heat-Driven Hydrothermal Flow at Yucca Mountain, Part I: Modeling and Analysis," *Nuclear Technology*, Vol. 104, No. 3, pp. 418–448 (1993).

9. Buscheck, T.A., and J.J. Nitao, "The Impact of Buoyant Gas-Phase Flow and Heterogeneity on Thermo-Hydrological Behavior at Yucca Mountain," American Nuclear Society, *Proceedings Fifth International High-Level Radioactive Waste Management Conference*, Las Vegas, NV, May 1994. Also, *UCRL-JC-115351*, Lawrence Livermore National Laboratory, Livermore, CA (1994).

10. Nitao, J.J., "V-TOUGH - An Enhanced Version of the TOUGH Code for the Thermal and Hydrologic Simulation of Large-Scale Problems in Nuclear Waste Isolation," *UCID-21954*, Lawrence Livermore National Laboratory, Livermore, CA (1989).

11. Pruess, K. "TOUGH User's Guide," *NUREG/CR-4645*, Nuclear Regulatory Commission (1987).

12. Peters, R.R., E.A. Klavetter, I.J. Hall, S.C. Blair, P.R. Hellers, and G.W. Gee, "Fracture and Matrix Hydrologic Characteristics of Tuffaceous Materials from Yucca Mountain, Nye County, Nevada," *SAND84-1471*, Sandia National Laboratories, Albuquerque, NM (1984).

13. Buscheck, T.A., J.J. Nitao, and D.A. Chesnut, "The Impact of Episodic Nonequilibrium Fracture-Matrix Flow on Geological Repository Performance," *Proceedings American Nuclear Society Topical Meeting on Nuclear Waste Packaging (Focus 91)*, Las Vegas, NV, Sept. 30–Oct. 2, 1991. Also, *UCRL-JC-106759*, Lawrence Livermore National Laboratory, Livermore, CA (1991).

14. DOE (U.S. Dept. of Energy), "Yucca Mountain Project Reference Information Base," *YMP/CC-0002 (Version 04.002)*, Nevada Operations Office, Las Vegas, NV (1990).

15. King, J., "Data Transmittal for Phase 2 Thermal Loading Study," Interoffice Correspondence, VA.SE.JK.5/93.031, prepared by Civilian Radioactive Waste Management System Management and Operating Contractor, TRW Safety Systems, Inc., Vienna, VA, May 24, 1993.

16. Weeks, E.P., "Gas-Phase Flow at Yucca Mountain," presentation to the National Academy of Sciences' Committee on the Technical Basis for Yucca Mountain Standards, *National Research Council*, December 16, 1993.

17. Weeks, E.P., personal communication, U.S. Geological Survey, Denver, CO (1993).

18. SNL (Sandia National Laboratories), "Site Characterization Plan - Conceptual Design Report," *SAND84-2641*, Sandia National Laboratories, Albuquerque, NM (1987).

19. Buscheck, T.A., D.G. Wilder, and J.J. Nitao, "Large-Scale *In Situ* Heater Tests for the Characterization of Hydrothermal Flow at Yucca Mountain," American Nuclear Society, *Proceedings Fourth International High-Level Radioactive Waste Management Conference*, Las Vegas, NV, April 1993. Also, *UCRL-JC-112445*, Lawrence Livermore National Laboratory, Livermore, CA (1993).

20. Buscheck, T.A., D.G. Wilder, and J.J. Nitao, "Repository-Heat-Driven Hydrothermal Flow at Yucca Mountain, Part II: Large-Scale *In Situ* Heater Tests," *Nuclear Technology*, Vol. 104, No. 3, pp. 449–471 (1993).